CHAPTER V
THE EFFECT OF VAPOR CORROSION INHIBITOR CONCENTRATION DOPED IN MAGNETIC PCH FOR PREPARATION OF POLYLACTIDE NANOCOMPOSITES AS AN ANTI-CORROSION PACKAGING

5.1 Abstract

The PCHs were synthesized by the self-assembly of silica framework around surfactant templates intercalated within the galleries of Na-montmorillonite clay to obtain PCH before it was modified the surface by ferric chloride hexahydrate and ferrous chloride tetrahydrate to obtain the magnetic PCH. Surface of magnetic PCH was modified by various VCI content to obtain magnetic PCH-VCIs. Magnetic PCH-VCIs were utilized as the inorganic filler in PLA nanocomposites. Polylactide/VCI modified magnetic PCH nanocomposites were prepared via direct melt intercalation by twin screw extruder. Polyethylene glycol was used as a plasticizer to improve the dispersion of VCI modified magnetic PCH in PLA matrix. Subsequently, the thin sheets were prepared by compression molding machine. The nanocomposites were characterized by using DSC and TG-DTA. The T_g and T_m of PLA/5% wt PEG were lower than those of neat PLA. The thermal properties of PLA nanocomposites insignificantly changed with higher magnetic PCH-VCIs content. The mechanical properties of PLA nanocomposite decreased with higher magnetic PCH-VCIs content due to the aggregation of magnetic PCH-VCIs. The PLA nanocomposite showed lower corrosion rate as compare with neat PLA.

keyword: porous clay heterostructures, polylactide, nanocomposites, vapor corrosion inhibitor.

5.2 Introduction

Polymer-clay nanocomposites have been a growing interest to development. Nanocomposites constitute a new class of material that involves nano-scale dispersion in a matrix. Nanocomposites have at least one ultrafine phase dimension, typically in the range of 1–100 nm, and exhibit improved properties when compared to micro- and macro-composites. Strong interfacial interactions between the

dispersed clay layers and the polymer matrix lead to enhanced mechanical, thermal and barrier properties of the virgin polymer [1]. The most commonly used clay to prepare nanocomposite is from the smectite group, such as montmorilonite (MMT). In this clay mineral the silicate layers are joined through relatively weak dipolar and Van der Waals forces and the cations Na^{+} and Ca^{2+} located in the interlayers. These cations can be replaced by organic cations such as alkylammonium ions through an ionexchange reaction to provide an organophilic silicate. Nanocomposite can be obtained by direct polymer melt intercalation, where polymer chains are spread into the space between the clay layers and this can be done by conventional polymer processing techniques such as extrusion [2].

Polylactide or poly (lactic acid) (PLA) is one of the most promising materials since it is thermoplastic, biodegradable, biocompatible and has high-strength, high-modulus and good processability [3]. PLA is a linear aliphatic thermoplastic which can either be synthesized by condensation of lactic acid or ring opening polymerization of lactide which is produced by fermentation of dextrose which it self is gained from annually renewable resources like corn [4].

Many research efforts focus on the polylactide-clay nanocomposites. The nanocomposites were prepared by melt compounding with polyethylene glycol (PEG) as a plasticizer. Plasticizers are one of the useful additional materials. Because plasticizers add to polymer matrix increase the flow ability, molecules of polymer matrix can easily intercalate between clay platelets [5].

The previous work in our group, surface PCH was modified by ferric chloride hexahydrate to induce the magnetic properties. These magnetic PCH were blended with polylactide for RFID application. From this point of view, one of the goals of this work is to modified surface of magnetic PCH by various VCI concentrations to induce the anti-corrosion properties, these as-synthesized mesoporous materials were blended with polylactide, and the properties concerning the capability of polylactide/magnetic PCH-VCIs nanocomposites. Furthermore, the anti-corrosion was investigated for anti-corrosion packaging.

5.3 Experimental

Materials

Montmorillonite (MMT) was provided by Pai Kong Nano Technology Co., Ltd. The cation exchange capacity (CEC) of MMT is 102 mmol/100g of clay.

Cetyltrimethylammonium [$C_{16}H_{33}N^{+}(CH_3)_3$] bromide (CTAB) was supplied by Fluka. Dodecylamine, $C_{12}H_{27}N$, (MW=185.35), (98% purified) was supplied by Aldrich. Tetraehtyl orthosilicate (TEOS), (MW=208.33), Ammonium hydroxide (NH_4OH), Ferric chloride hexahydrate ($FeCl_3.6H_2O$) and Ferrous chloride tetrahydrate ($FeCl_2.4H_2O$) were purchased from Fluka. Methanol (CH_3OH) was supplied by Lab Scan and Hydrochoric acid (HCl) was supplied by Carlo Erba. Vapor corrosion inhibitor (VCI 609) was provided by Optimal Technology Co., Ltd.

Polylactide 4042D (PLA) was supplied by NatureWorks Co., Ltd and Polyethylene glycol (PEG) was supplied by Sigma.

Purification and pH Adjustment of Na-Monmorillonite

Na-Monmorillonite was pulverized and sieve through 325 mesh. Three 10-g of the passing part were purified by centrifugation and then washed with distilled water until the pH value is near 7. After that, centrifugation was applied. Again, the same amount of distilled was added, and then the pH of each sample was adjusted to 9.0 by using dilute HCl and NaOH solutions. This procedure was repeated for 48 h to equilibrate the pH of each sample. The samples were air-dried overnight and again pulverized in a mortar.

Synthesis of Porous Clay Heterostructures (PCHs)

Na-Monmorillonite was converted into a Quqternary ammonium exchange form by ion exchange with cetyltrimethylammonium bromide and stirred at 50 °C for 24 h. After the reaction time, the solid was filtered out, washed with a mixture of methanol and water and then air-dried. The obtained organoclay was stirred in dodecylamine for 30 min at 50°C following which TEOS was added (at molar ratio of organoclay:dodecylamine:TEOS was 1:20:200). The resulting suspension was stirred for further 4 h at room temperature. The solid was separated from solution

again by filtration and air-dried overnight at room temperature to form the as-synthesized PCH. The surfactant was removed from the as-synthesized PCH by solvent extraction using methanol/HCL solution. Typically, 1 g of the as-synthesized PCH material has been added to 45 mL of methanol and 5 mL of HCl and refluxed for 2 h. The solid was subsequently filtrated out and washed with a mixture of methanol and water and air-dried at room temperature overnight.

Preparation of Magnetic PCHs

Ferric chloride hexahydrate and ferrous chloride tetrahydrate at 20 wt% were used as iron sources which they were added in PCH. Aqueous ammonia was used as the precipitator. Distilled water was used as the solvent. Before the reaction, N_2 gas was flown through the reaction medium. The reaction was operated in a closed system to provide a nonoxidation environment. NH_4OH was slowly injected into PCH which added ferric chloride hexahydrate and ferrous chloride tetrahydrate under stirring 30 min. The dispersion was centrifuged at 3000 rpm for 20 min. After precipitation, the Fe_2O_3 particles in PCH were repeatedly washed and filtered before drying at room temperature in air atmosphere to form powders.

Preparation of Magnetic PCH-VCI

Vapor corrosion inhibitor was add in magnetic PCH at 20, 40, 60, and 80 wt% and stirred in ethanol which is used as the solvent at 50 °C for 30 min. The reaction was operated in a closed system to protect a volatility of VCI. After the reaction time, the solid was filtered out, washed with a mixture of methanol and water and then air-dried to form powders

Preparation of Nanocomposites

VCI 20, 40, 60, and 80 %wt, Magnetic PCH 1%wt, PEG 5 wt% and PLA were melt blended in a co-rotating twin-screw extruder (Lab tech) with L/D=40/1 and D=20 mm; the processing conditions were the following: temperature (°C): 80, 150, 150, 160, 160, 165, 165,170,170, and 175°C from hopper to die, respectively and the screw rotation is 50 rpm. Each composition was premixed in a tumble mixer before introducing into the twin-screw extruder to be well mixed and extruded

through a single strand die, and solidified with cold water and pelletized. The obtained pellet was dried in oven.

Fabrication of Thin Sheet Nanocomposites

The nanocomposites films were prepared by compression molding machine. The nanocomposites pellets were dried in oven prior to compress. The compression molding was performed by using a Wabash V50H Press, at 195°C for 10 minutes and 25 tons compression force for 15 minutes before being cooled down to 50°C and thickness in the range of 0.1–0.3 mm.

Physical Measurements

TG-DTA curves were collected on a Perkin-Elmer Pyris Diamond TG/DTA instrument. The sample was loaded on the platinum pan and heated from 30°C to 500°C at a heating rate of 10°C/min under N_2 flow.

DSC analysis were carried out using a Perkin-Elmer DSC 7 instrument. The sample was first heated from 30°C to 180°C and cooled down at a rate of 10°C/min under a N_2 atmosphere with a flow rate of 60 ml/min. The sample was then reheated to 180°C at the same rate.

The volatilization of VCI test carried out by placing the samples in a jar about 15 g, with an airtight lid holding the litmus paper.

Corrosion Test was investigated according to the Federal Standard No.101C, Method 4031 with a few modifications. The carbon steel test specimens were polished with the emery paper and were inserted in sealed film packages, and then submitted to the chamber. The chamber was a glass jar containing 45 ml of water/glycerin solution, with an airtight lid holding the carbon steel specimens.

Tensile Strength, elongation at break, stiffness and Young's modulus were measured according to ASTM D 882-91 using a LLOYD Mechanical Universal Testing Machine with a 500 N load cell, a 10.00 mm/min crosshead speed and a gauge length 50 mm. Test sample was cut into rectangular shape with a size of 10 x 150 mm and thickness in the range of 0.1-0.25 mm.

5.4 Results and Discussion

5.4.1 Characterization of magnetic PCH-VCIs

A. The volatilization of PCH, Magnetic PCH and Magnetic PCH-VCIs

The volatilization of PCH, Magnetic PCH, Magnetic PCH-VCIs and Pure VCI provided in Figure 5.1 (before test) and Figure 5.2 (after test). The Litmus paper of both PCH and Magnetic PCH do not change the color. After magnetic PCH was modified by VCI to obtain Magnetic PCH-VCIs, the Litmus papers were gradually changed the color from pH 7 to pH8. This suggested that the volatilization of VCI can occur in the clay.

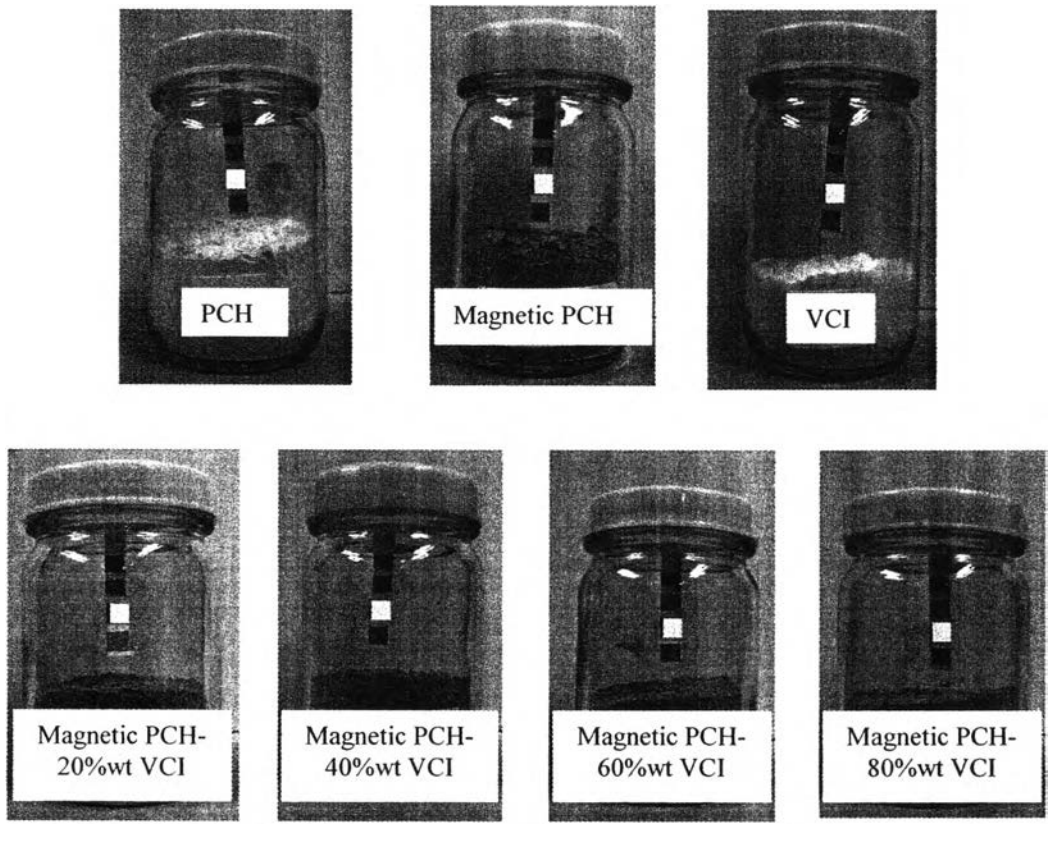

Figure 5.1 Volatilization before test of PCH, magnetic PCH, Pure VCI, and Magnetic PCH-VCIs.

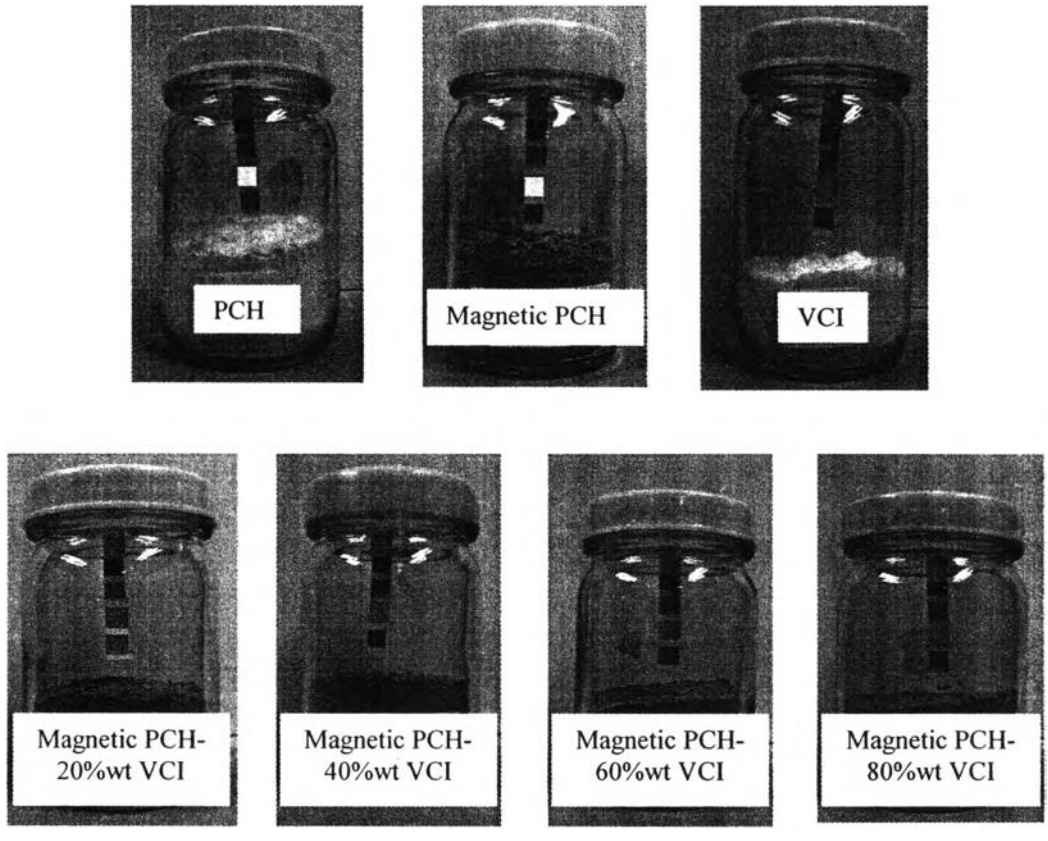

Figure 5.2 Volatilization after test of PCH, magnetic PCH, Pure VCI, and Magnetic PCH-VCIs.

B. The Corrosion Test of PCH, Magnetic PCH and Magnetic PCH-VCIs

The corrosion test (86.5% RH at 20°C) of PCH, Magnetic PCH, Magnetic PCH-VCIs and Pure VCI provided in Table 5.1, Figure 5.3, Figure 5.4 (before test) and Figure 5.5 (after test). The carbon steel specimen in PCH test had been corroded after 35 day and the carbon steel specimen in Magnetic PCH test had been corroded after 50 day. This suggested that Magnetic PCH can protect the corrosion better than PCH because Magnetic PCH can absorb moisture higher than PCH according to the moisture absorption test.

The carbon steel specimen in Pure VCI test had been corroded after 61 day and the carbon steel specimen in Magnetic PCH-20, 40, 60 and 80%wt VCI test had been corroded after 79, 85, 73 and 70 day, respectively. This revealed that the incorporation of VCI on magnetic PCH led to lower corrosion rate because of the volatilization of VCI, possible due to the development of new magnetic PCH-VCI

interactions which are weaker than intermolecular interaction of pure VCI [6]. The outer surface of carbon steel is composed of metal oxide. VCI attaches itself to oxide through weak chemical bonding and forms an adsorbed monolayer to shield this interface from penetration by corrosive agents such as water [7].

Table 5.1 The first date of corrosion of carbon steel in PCH, Magnetic PCH, Pure VCI and Magnetic PCH-VCIs

Sample	The first date$^{(th)}$ of corrosion
PCH	35
Magnetic PCH-0%wt VCI	50
Magnetic PCH-20% wt VCI	79
Magnetic PCH-40% wt VCI	85
Magnetic PCH-60%wt VCI	73
Magnetic PCH-80%wt VCI	70
Pure VCI	61

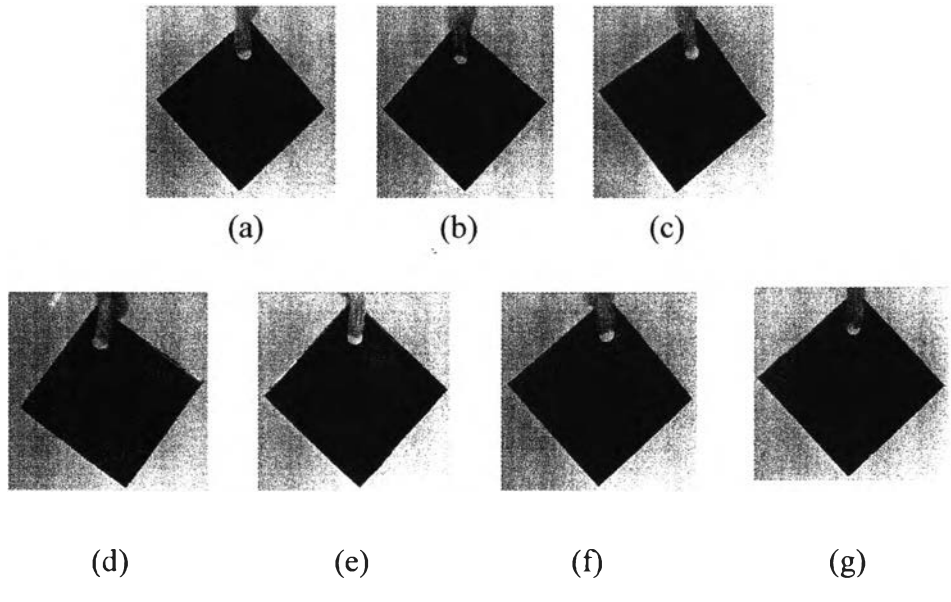

Figure 5.3 The carbon steel after corrosion test (86.5% RH at 20°C) of (a) PCH, (b) Magnetic PCH, (c) Pure VCI, (d) Magnetic PCH-20%wt VCI, (e) Magnetic PCH-40%wt VCI, (f) Magnetic PCH-60%wt VCI, and (g) Magnetic PCH-80%wt VCI.

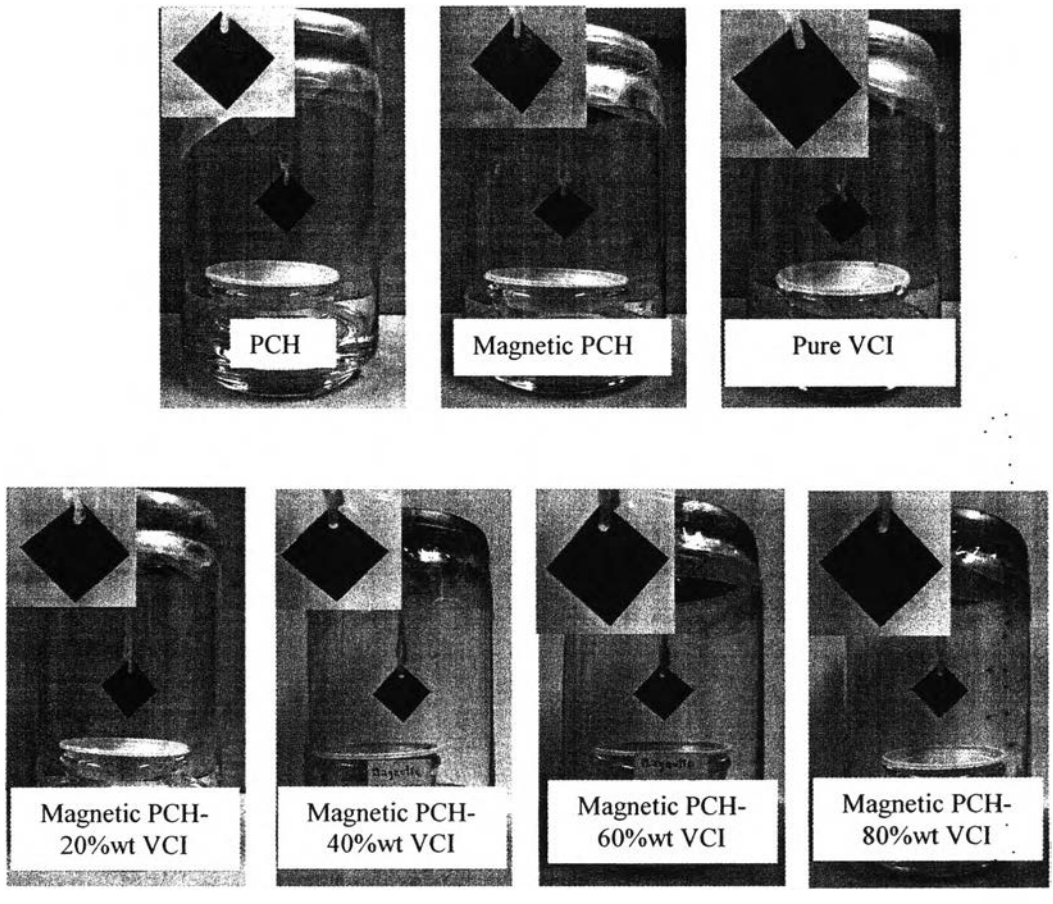

Figure 5.4 The corrosion before test (86.5% RH at 20°C) of PCH, magnetic PCH, Pure VCI, and Magnetic PCH-VCIs.

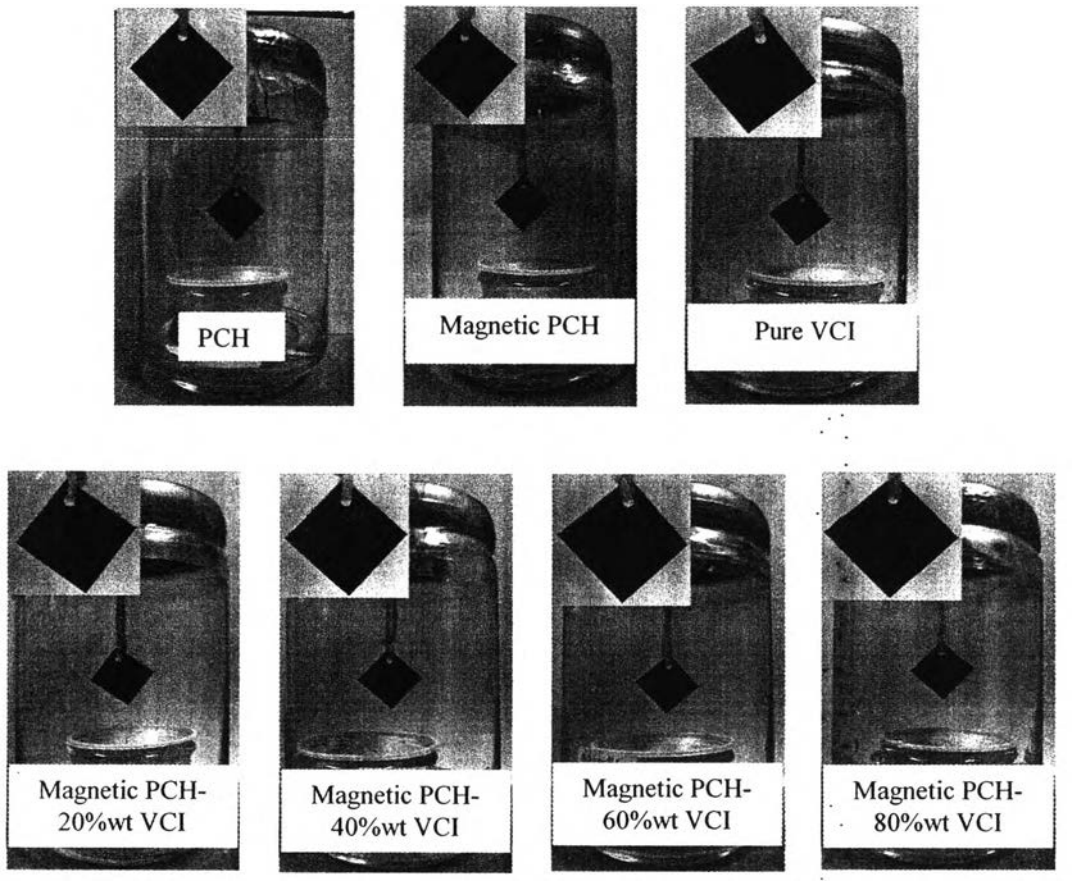

Figure 5.5 The corrosion after test (86.5% RH at 20°C) of PCH, magnetic PCH, Pure VCI, and Magnetic PCH-VCIs.

5.4.2 Characterization of PLA Nanocomposites

A. Thermal Properties of Nanocomposites

Melting temperatures of PLA and PLA nanocomposites are observed by DSC heating scan thermograms in Table 5.2 and Figure 5.6. The neat PLA showed glass transition temperature (T_g) at 64.0°C and the melting temperature(T_m) at 142.4°C. After blending PLA with PEG as the plasticizer, the T_g and T_m of PLA/ 5%wt PEG were lower than neat PLA. The T_g and T_m of PLA nanocomposites with various VCI contents in magnetic PCH insignificantly changed with the higher content of VCI in magnetic PCH. All results of thermal properties are listed in Table 5.2 and Figure 5.6–5.7.

Table 5.2 Thermal properties of neat PLA and PLA nanocomposites

Sample	T_g (°C)	T_m (°C)	T_d (°C)	Char residue at 500 (°C)
PLA	64.0	142.4	345.3	1.3
PLA/ 5%wt PEG	46.6	139.9	334.0	1.6
PLA/ 5%wt PEG/ 1%wt PCH	51.0	142.7	332.6	1.7
PLA/ 5%wt PEG/ 1%wt magnetic PCH- 0%wt VCI	49.6	142.2	296.1	5.8
PLA/ 5%wt PEG/ 1%wt magnetic PCH- 20%wt VCI	48.6	141.2	298.6	6.1
PLA/ 5%wt PEG/ 1%wt magnetic PCH- 40%wt VCI	48.9	141.7	299.2	6.8
PLA/ 5%wt PEG/ 1%wt magnetic PCH- 60%wt VCI	48.7	141.5	300.7	7.0
PLA/ 5%wt PEG/ 1%wt magnetic PCH- 80%wt VCI	48.9	141.8	302.9	7.2
PLA/ 5%wt PEG/1 %wt VCI	45.3	139.7, 147.6	322.8	2.3

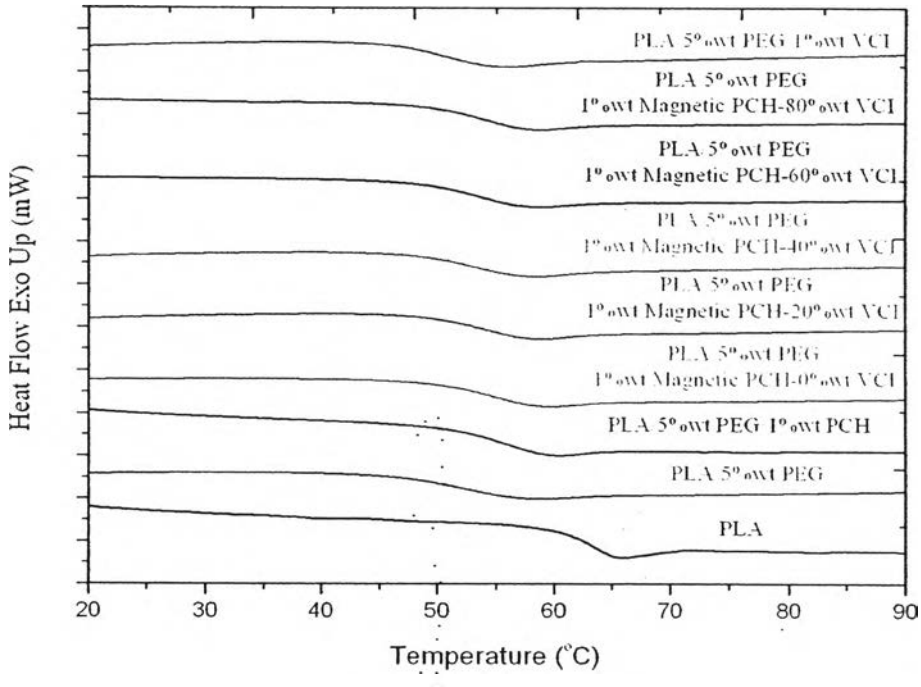

(a)

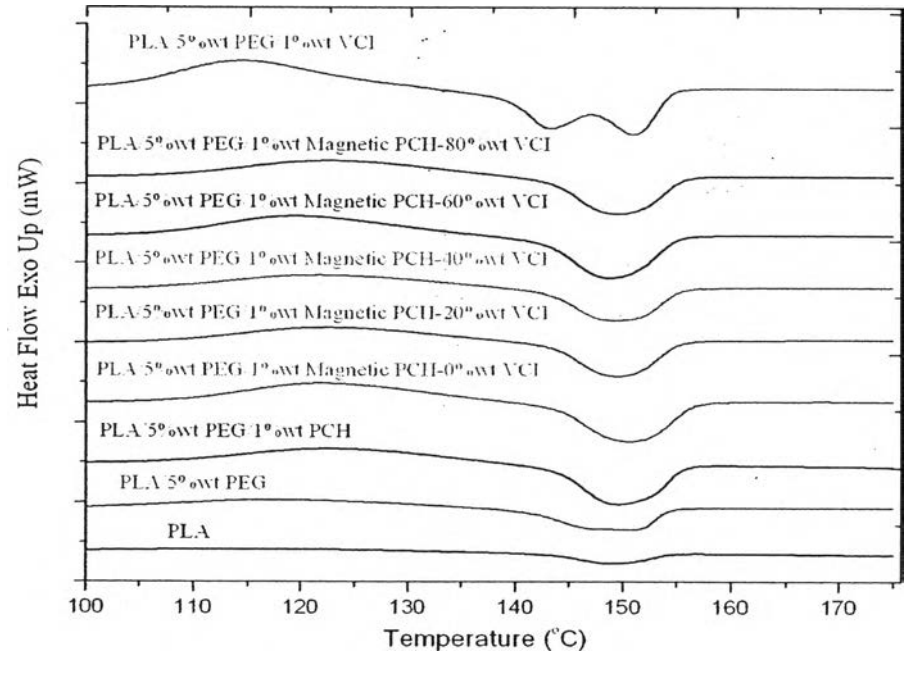

(b)

Figure 5.6 DSC heating scan thermograms of neat PLA, PLA/5%wt PEG and various PLA nanocomposites (a) Glass transition temperature, and (b) Melting temperature.

TG-DTA curves of PLA and the nanocomposites are shown in Figure 5.7(a). The thermal degradation of PLA and all nanocomposites occured in single stage, and it indicated that thermal stability of the PLA nanocomposites were decreased when compared to neat PLA. The PLA nanocomposites marginally increased with the higher content of VCI in magnetic PCH. Generally, the shift considerably towards higher temperature may be attributed to the formation of a high-performance carbonaceous-silicate char, builds up on the surface [8].

As shown in Figure 5.7 (b), the incorporation of VCI on magnetic PCH led to a shift in the DTG peaks to lower temperature. The DTG temperature peaks are observed to be directly proportional to the amount of VCI adsorbed, being lowest at 20 % wt VCI and converging to the higher temperatures of the pure VCI. This is regarded as an indication of an increase in volatility brought about by the incorporation on the magnetic PCH, possible due to the development of new magnetic PCH-VCI interactions which are weaker than intermolecular interaction of pure VCI [6].

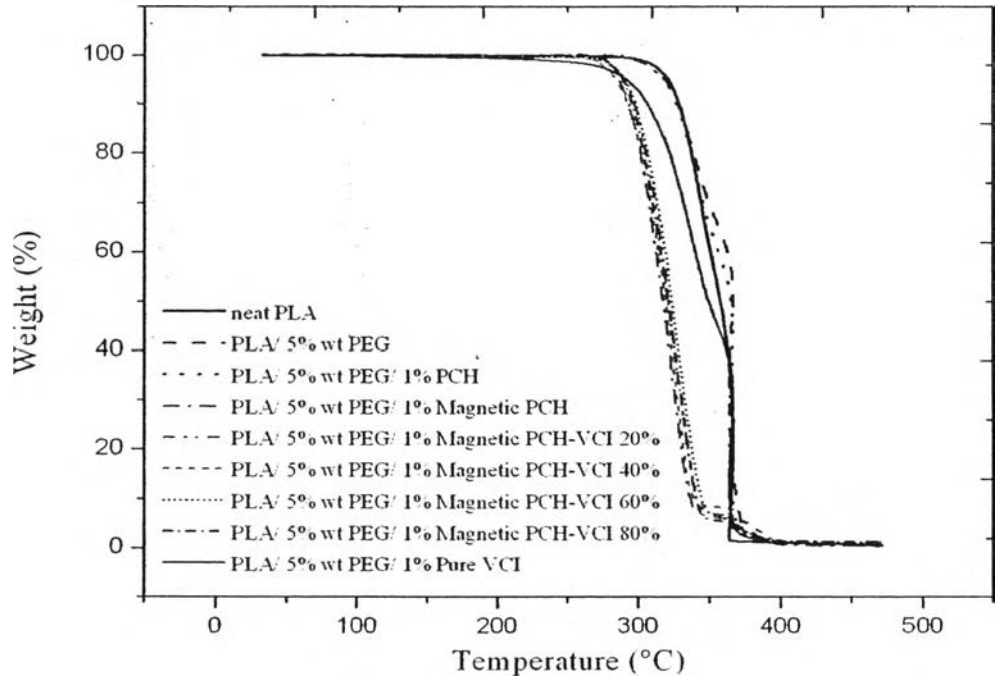

(a)

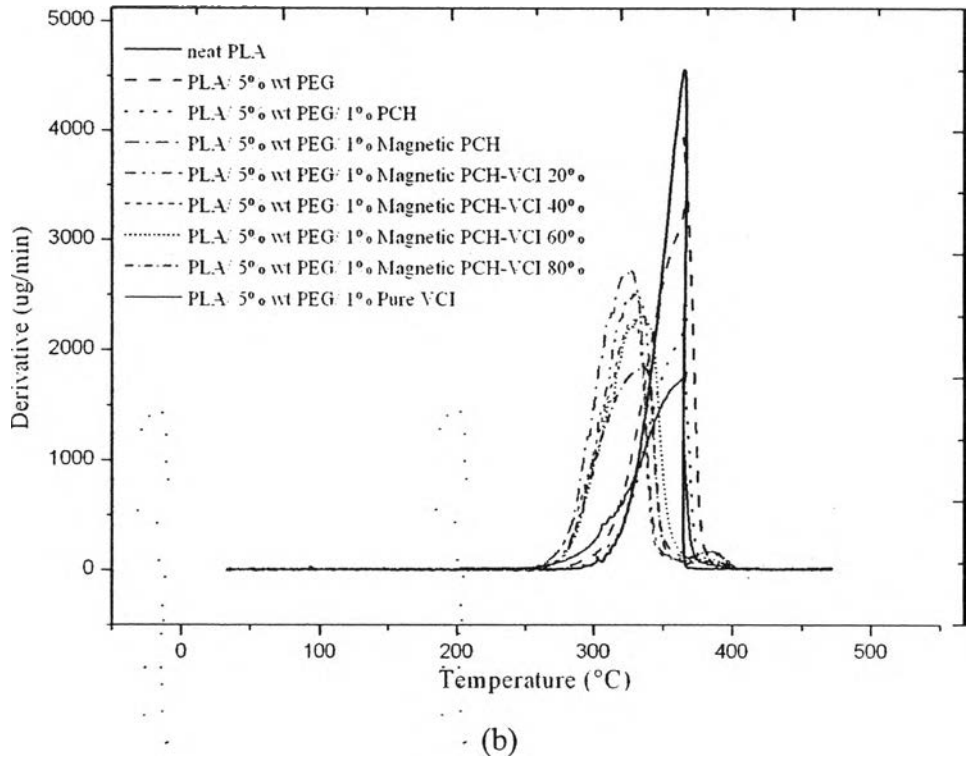

Figure 5.7 TG-DTA curves (a), and DTG temperature peak (b) of neat PLA, PLA/5%wt PEG and PLA nanocomposites.

B. Mechanical measurement of PLA nanocomposites

The mechanical properties of neat PLA and PLA nanocomposites are shown in Table 5.3 and Figure 5.8. Tensile strength, young's modulus and % elongation at break of PLA nanocomposites decreased with the higher content of VCI in magnetic PCH. However, % elongation at break increased when compare with neat PLA due to the effect of PEG which act as plasticizer. The aggregation of magnetic PCH-VCIs affect to the mechanical properties of nanocomposites and the obstruction of magnetic PCH-VCIs to the movement of PLA matrix was a reason in decline of mechanical properties with increasing VCI content which propably leads to lower polymeric chain mobility.

Table 5.3 Mechanical Properties of neat PLA and PLA nanocomposites

Sample	Tensile strength (MPa)	Elongation at Break (%)	Young's Modulus (MPa)
PLA	9.32 ± 1.20	3.38 ± 0.15	2641.89 ± 85.70
PLA/5%wt PEG	9.93 ± 0.80	4.53 ± 0.33	1751.49 ± 99.42
PLA/5%wt PEG/1% wt PCH	8.21 ± 0.97	4.77 ± 0.39	1999.76 ± 79.52
PLA/5%wt PEG/1% wt Magnetic PCH-0% wt VCI	9.16 ± 0.44	4.37 ± 0.34	2003.77 ± 68.53
PLA/5%wt PEG/1% wt Magnetic PCH-20% wt VCI	8.93± 0.24	4.28 ± 0.20	2114.77 ± 77.70
PLA/5%wt PEG/1% wt Magnetic PCH-40% wt VCI	8.58 ± 0.51	4.18 ± 0.20	1915.89 ± 83.68
PLA/5%wt PEG/1% wt Magnetic PCH-60% wt VCI	8.31 ± 0.80	4.08 ± 0.20	1881.39 ± 95.62
PLA/5%wt PEG/1% wt Magnetic PCH-80% wt VCI	7.95 ± 0.36	3.99 ± 0.30	1753.00 ± 83.33

*PLA/5%wt PEG/1% wt VCI cannot fabricate to the thin sheet.

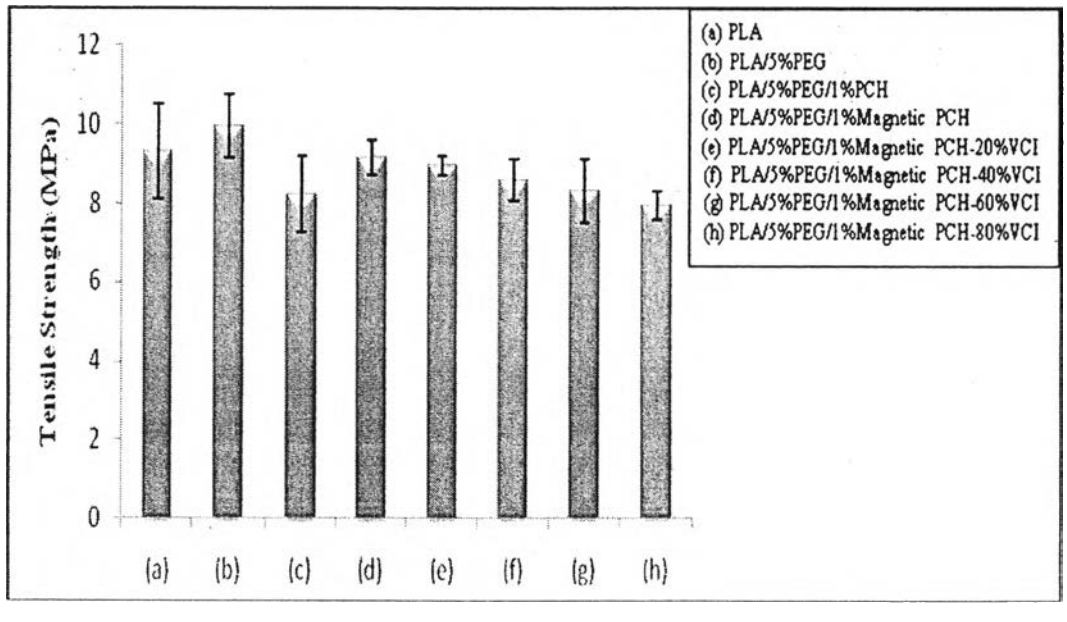

(a)

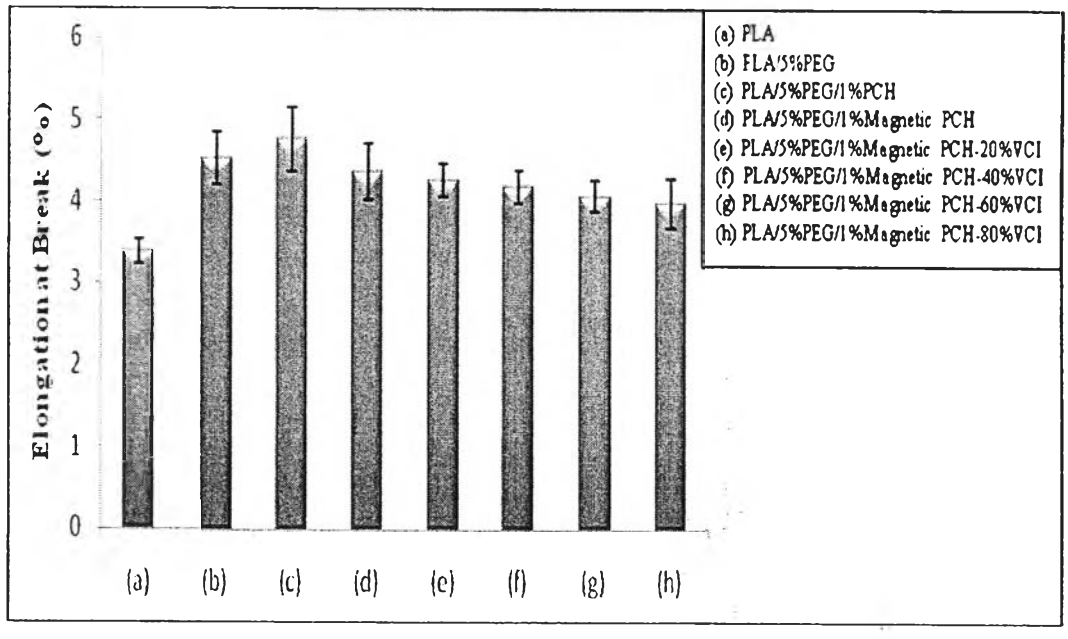

(b)

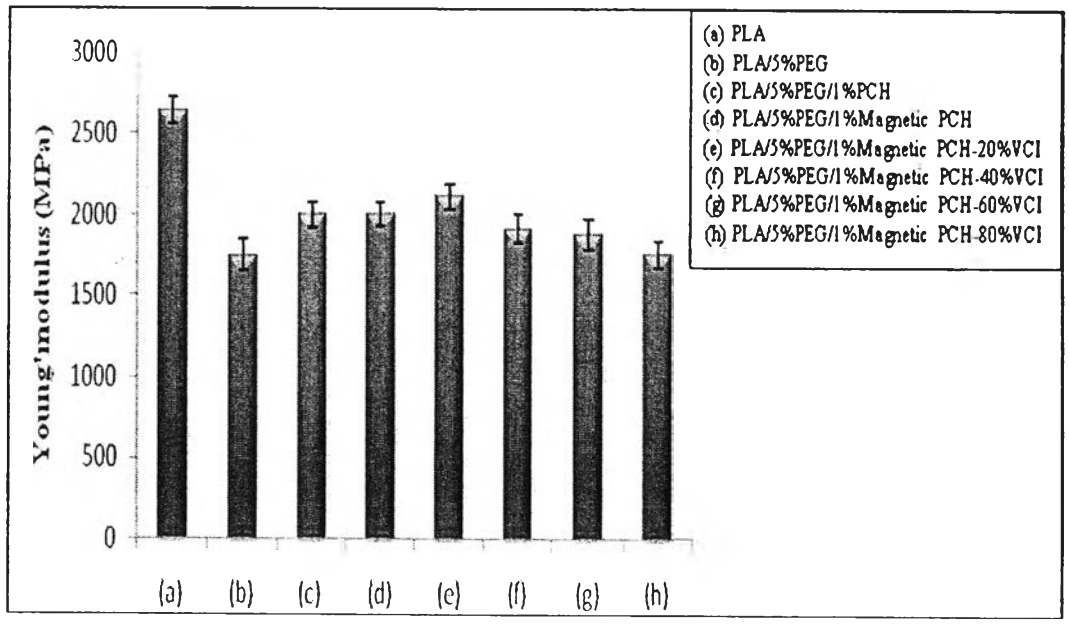

(c)

Figure 5.8 Mechanical Properties of neat PLA and PLA nanocomposites (a) Tensile Strength, (b) % Elongation at Break, and (c) Young's Modulus.

C. The Corrosion Test of PLA Nanocomposites

The corrosion test (86.5% RH at 20°C) of neat PLA and PLA nanocomposites were provided in Table 5.4, Figure 5.9, Figure 5.10 (before test) and Figure 5.11 (after test). The carbon steel specimen in neat PLA test had been corroded after 5 day. The carbon steel specimen in Pure VCI test had been corroded after 11 day and the carbon steel specimen in PLA nanocomposites test had lower corrosion rate because of the volatilization of VCI, possible due to the development of new magnetic PCH-VCIs interactions which are weaker than intermolecular interaction of pure VCI [6]. The outer surface of carbon steel is composed of metal oxide. VCI attaches itself to oxide through weak chemical bonding and forms an adsorbed monolayer to shield this interface from penetration by corrosive agents such as water [7].

Table 5.4 The first date of corrosion of carbon steel in neat PLA and PLA nanocomposites

Sample	The first date$^{(th)}$ of corrosion
PLA	5
PLA/ 5%wt PEG	6
PLA/ 5%wt PEG/ 1%wt PCH	6
PLA/ 5%wt PEG/ 1%wt magnetic PCH-0%wt VCI	9
PLA/ 5%wt PEG/ 1%wt magnetic PCH-20%wt VCI	12
PLA/ 5%wt PEG/ 1%wt magnetic PCH-40%wt VCI	18
PLA/ 5%wt PEG/ 1%wt magnetic PCH-60%wt VCI	16
PLA/ 5%wt PEG/ 1%wt magnetic PCH-80%wt VCI	15
PLA/ 5%wt PEG/ 1%wt VCI	11

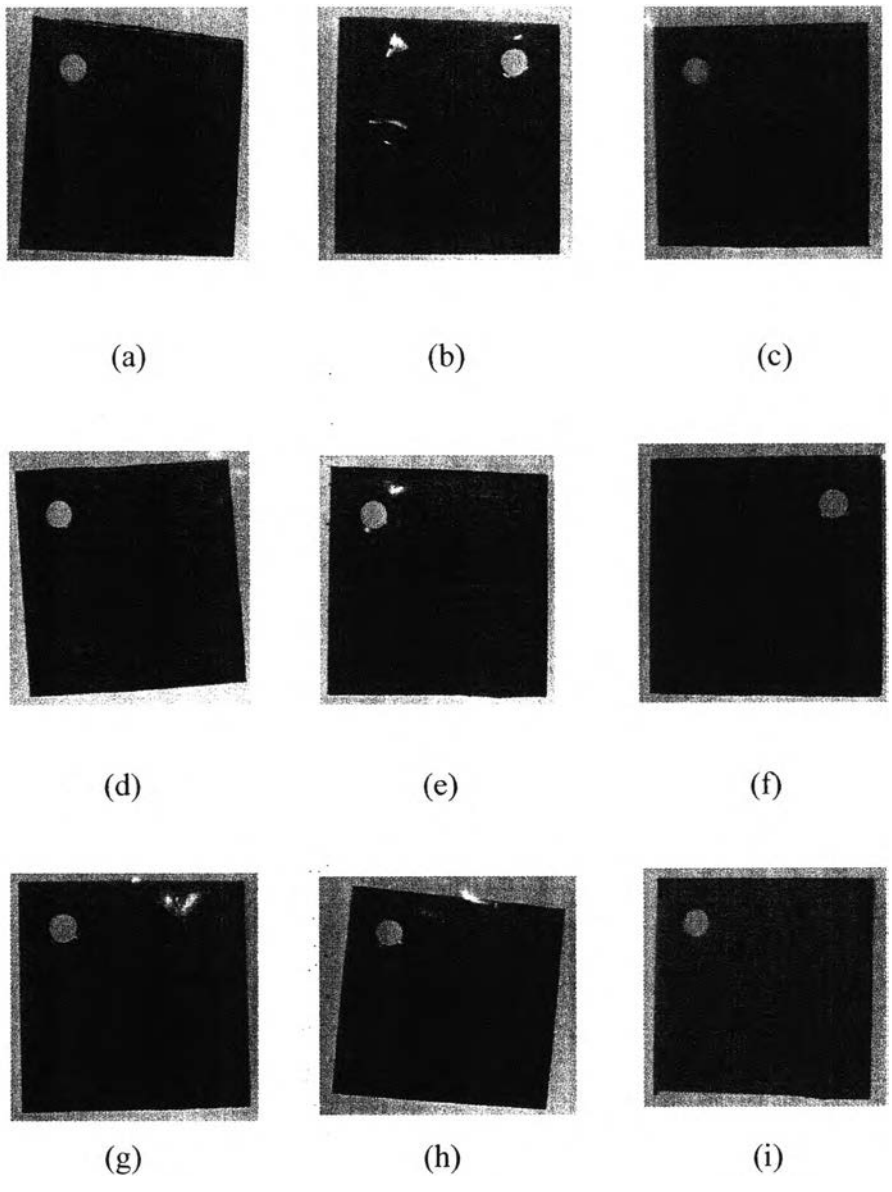

Figure 5.9 The carbon steel after corrosion test (86.5% RH at 20°C) of nanocomposites (a) neat PLA, (b) PLA/5%wt PEG,(c) PLA/5%wt PEG/1%wt PCH, (d) PLA/5%wt PEG/1%wt Magnetic PCH-0%wt VCI, (e) PLA/5%wt PEG/1%wt Magnetic PCH-20%wt VCI (f) PLA/5%wt PEG/1%wt Magnetic PCH-40%wt VCI, (g) PLA/5%wt PEG/1%wt Magnetic PCH-60%wt VCI, (h) PLA/5%wt PEG/1%wt Magnetic PCH-80%wt VCI, and (i) PLA/5%wt PEG/1%wt VCI.

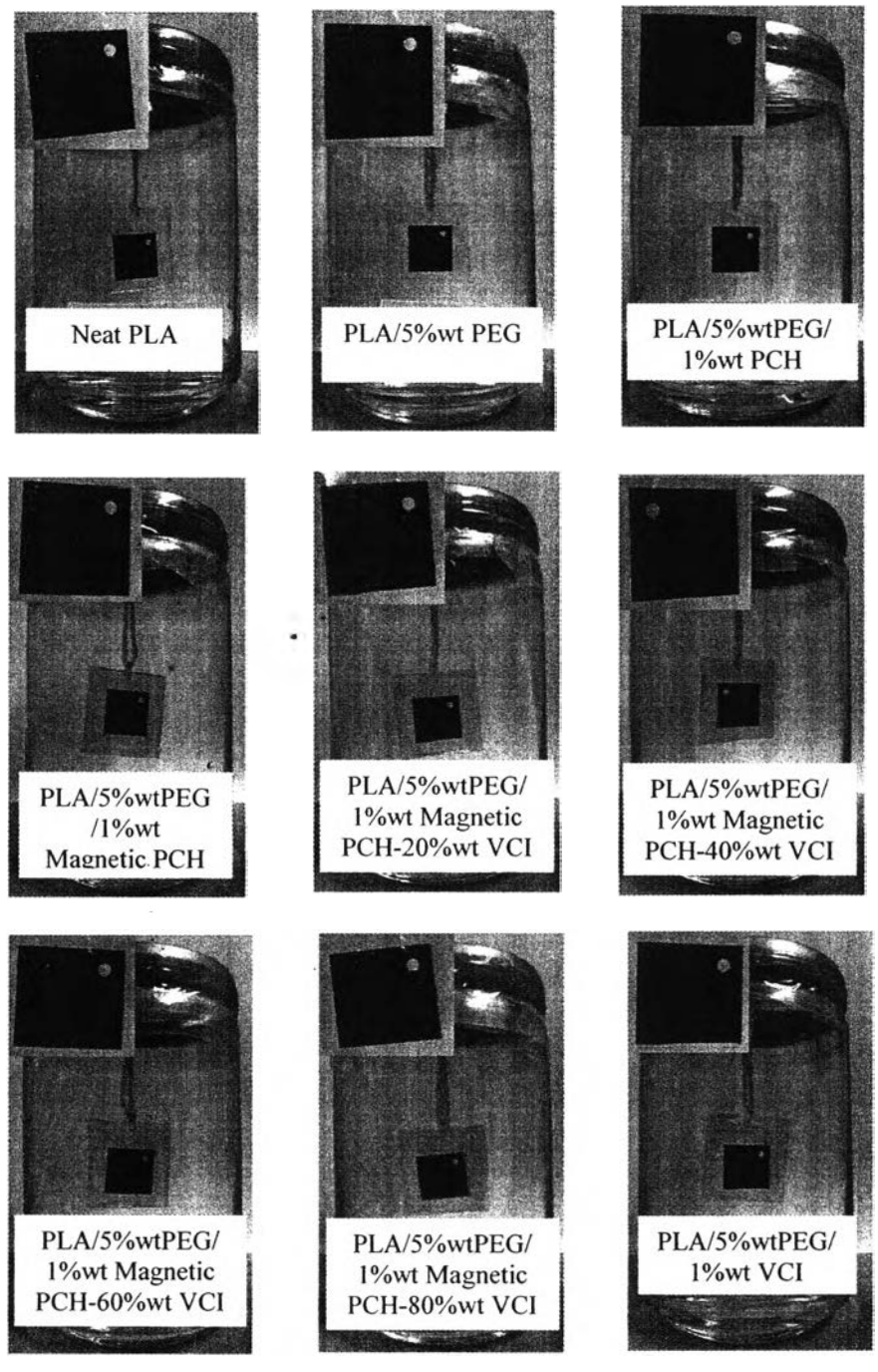

Figure 5.10 The corrosion before test (86.5% RH at 20°C) of neat PLA and PLA nanocomposites with various VCI contents.

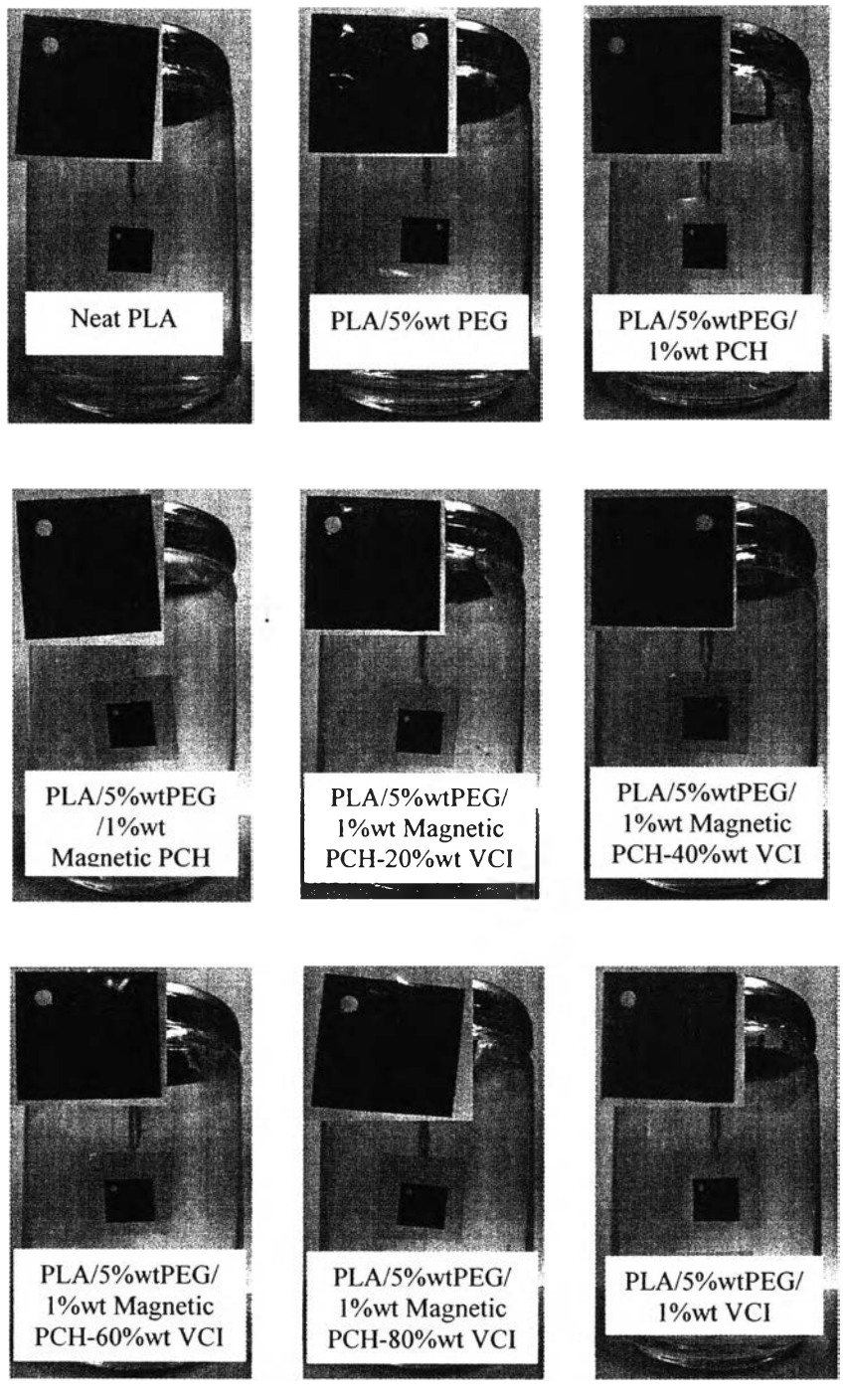

Figure 5.11 The corrosion after test (86.5% RH at 20°C) of neat PLA and PLA nanocomposites with various VCI contents.

5.5 Conclusions

PCH was modified the surface by ferric chloride hexahydrate and ferrous chloride tetrahydrate to obtain the magnetic PCH. Then, surface of magnetic PCH was modified by various VCI content to obtain magnetic PCH-VCIs. These materials were blend with polylactide via direct melt intercalation method by twin screw extruder. Polyethylene glycol was used as a plasticizer to improve the dispersion of VCI modified magnetic PCH in PLA matrix. Subsequently, they were fabricated to thin sheet by compression molding machine. The thermal properties of PLA nanocomposites insignificantly changed with the higher content of VCI in magnetic PCH. Tensile strength, young's modulus and % elongation at break of PLA nanocomposites decreased with the higher content of VCI in magnetic PCH. However, % elongation at break increased when compare with neat PLA. From the corrosion test, the PLA nanocomposite showed lower corrosion rate as compare with neat PLA and the incorporation of 40%wt VCI on magnetic PCH showed the lowest corrosion.

5.6 Acknowledgements

This work is funded by National Research Council of Thailand (NRCT). The authors would also thank Polymer Processing and Polymer Nanomaterial Research Unit and the Center of Excellence for Petroleum, Petrochemical, and Advanced Materials, Thailand for their partially funding.

5.7 References

[1] Ishii, R., Nakatsuji, M., and Ooi, K. Micropor. Mesopor. Mater. 79 (2005) 111.

[2] Galarneau, A., Barodawalla, A., and Pinnavaia, T.J. Nature 374 (1995) 529.

[3] Drumright, R.E., Gruber, P.R., and Henton, D.E Advanced Materials 12 (2000) 1841.

[4] Bax, B., Mussig, J. Composites Science and Technology 68 (2008) 1607.

[5] Shui Tanoue, Aniwat Hasook, Yoshiyuki Iemoto Department of Materials Science and Engineering, University of Fukui, 3-9-1 Bunkyo, Fukui 910-8507, Japan

[6] L.R.M. Estevao, R.S.V. Nascimento. Corrosion Science., 43., 1133-1153

[7] Da-quan Zhang, Zhong-xun An, Qing-yi Pan, Li-xin Gao, Guo-ding Zhou. Applied Surface Science 253 (2006) 1343–1348.

[8] Modesti, M., Lorenzetti, A., Bon, D., and Besco, S. Polymer Degradation and Stability 91 (2006) 672.

[9] Meneghetti, P. and Qutubuddin, S. Thermochimica Acta (2006) *In Press.*

[10] Arau´jo, E.M., Me´lo, T.J.A., Santana, L.N.L., Neves, G.A., Ferreira, H.C.,Lira, H.L., Carvalho, L.H., A'vila Jr., M.M., Pontes, M.K.G., and Arau´jo, I.S., Materials Science and Engineering B 112 (2004) 175.

[11] Lertwimolnun, W., and Vergnes, B. Polymer 46 (2005) 3462.

[12] Shah, R.K., Hunter, D.L. and Paul, D.R. Polymer. 46 (2005) 2646.

[13] Sinha Ray, S., and Okamoto, M. Prog. Polym. Sci. 28 (2003) 1539.

[14] LeBaron, P.C., Wang, Z., and Pinnavaia, T.J., Applied Clay Science 15 (1999) 11.

[15] Seephueng, A., Magaraphan, R., Nithitanakul, M., and Manuspiya, H. Proceeding of the 14 th PPC Symposium on Petroleum, Petrochems, and Polymers, (2008).

[16] Polverejan, M., Liu, Y., and Pinnavaia, T.J. Chem. Mater. 14 (2002) 2283.

[17] Zhu, H.Y., Ding, Z., and Barry, J.C. J. Phys.Chem. B. 106 (2002) 11420.

[18] Ramos Filho, F.G., Melo, T.A., Rabello, M.S., and Silva, S.M., Polymer Degradation and Stability 89 (2005) 383.

[19] Perrin-Sarazin, F., and Ton-That, M.T., Bureau, M.N., and Denault, J., Polymer 46 (2005) 11624.

[20] Alexandre, M. and Dubois, P. Materials Science and Engineering 28 (2000) 63.